Proceedings of the ASME 2016 Dynamic Systems and Control Conference
DSCC2016
October 12-14, 2016, Minneapolis, Minnesota, USA

DSCC2016-9714

REDUCED ORDER MODEL ON DC BIAS EFFECT ON THE FREQUENCY RESPONSE OF ELECTROSTATICALLY ACTUATED BIOSENSOR MICROPLATES

Dumitru I. Caruntu
Mechanical Engineering Department
The University of Texas Rio Grande Valley
Edinburg, Texas 78539

Christian Reyes
Mechanical Engineering Department
The University of Texas Rio Grande Valley
Edinburg, Texas 78539

ABSTRACT

This paper investigates the frequency response of microplates under electrostatic actuation. The microplate is parallel to a fixed ground plate. The electrostatic force that actuates the system is given by both Alternate Current (AC) and Direct Current (DC) voltages. The AC frequency is set to be near half natural frequency of the structure. Damping influence is also investigated in this paper. The method of investigation is Reduced Order Model. The effects of various parameters on the response of the structure are reported.

INTRODUCTION

In the past decade microelectromechanical systems have gained large popularity among the research community. These devices offer many benefits over other devices including cost effect manufacturing, size advantage, and low power requirements. These devices also have many different applications in various fields, the most popular application being sensors [1].

In order to take advantage of the possible applications these devices can serve it is crucial to understand the behavior and phenomena occuring at the micro scale [2-10]. A very important phenomenon that needs to be understood is pull-in effect, where in the case of cantilevers the system experiences instability and collapses to the ground plate. Talebian *et al.* [2] examined the pull-in voltage and frequency response of an electrostatically actuated micro plate and the effect temperature has on the system. The paper uses the Kirchhoff thin plate theory to derive the equation of motion and linearizes it using the step-by-step linearization method (SSLM). The results obtained showed the change in pull-in voltage at different operating temperatures. The paper concludes that at colder operating temperatures the pull-in voltage is higher than at warmer temperatures. Aside from understanding the phenomena that occurs at the micro scale, it is also important to understand the behavior the system exhibits. Caruntu and Taylor [8] investigated the behavior of a MEMS resonator that was electrostatically actuated with soft AC and DC voltage. The electrostatic actuation sets the resonator into a nonlinear parametric resonance. The method of multiple scales (MMS) is used to model the resonator and the results are validated using reduced order model (ROM). The results obtained showed that with the DC voltage added the bifurcation point is shifted to higher amplitudes and lower frequencies. Something else that is important to keep in mind when examining the behavior is the parameters affecting the system. Investigations of these parameters can determine how much of an impact they have on the overall system. Li *et al.* [11] examined an electrostatically actuated microplate under hydrostatic pressure. In their model they included both the effect of electrostatic force and hydrostatic pressure. An energy equivalent method was used to model the microplate and analyze the resonant frequency. Their results showed that for small amplitudes the resonant frequency can be decreased from the influence of electrostatic force and hydrostatic pressure. The results obtained were also validated using finite element method.

In this paper the effect of AC and DC electrostatic actuation on a microplate is investigated. The reduced order model (ROM) method is used to investigate the influences of damping, AC and DC voltage.

SYSTEM MODEL

The MEMS system consist of two parallel circular plates. The top plate is fixed from the edges and is deformable while the bottom plate (electrode) is rigid as shown in Fig. 1.

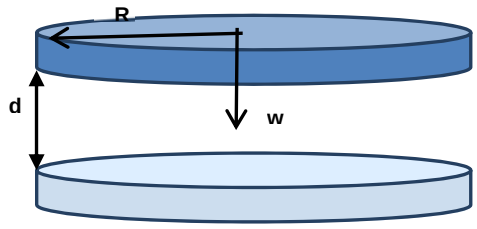

Fig. 1. MEMS circular plate suspended above ground plate

DC voltage is between these two plates as well as AC voltage at a frequency near half natural frequency of the top plates. The AC voltage causes a parametric resonance of the top flexible plate. *R* is the radius of the circular plates, *d* is the gap length between the plates, and *w* is the dimensionless deflection of the top plate. The dimensionless equation of motion of axisymmetric vibrations of circular plates is given by

$$\frac{\partial^2 w}{\partial t^2}+\mu\frac{\partial w}{\partial t}+\frac{\partial^4 w}{\partial r^4}+\frac{2}{r}\frac{\partial^3 w}{\partial r^3}-\frac{1}{r^2}\frac{\partial^2 w}{\partial r^2}+\frac{1}{r^3}\frac{\partial w}{\partial r}=\frac{(\sqrt{\delta_{OD}}+\sqrt{\delta_{OA}}\cos\Omega t)^2}{(1-w)^2} \tag{1}$$

where *t* is the dimensionless time, *r* is the dimensionless position from the center of the plate, and *w* is the dimensionless deflection of the top plate given by

$$w=\frac{\hat{w}}{d},\quad r=\frac{\hat{r}}{R},\quad t=\hat{t}\sqrt{\frac{D}{\rho h R^4}} \tag{2}$$

and where $\hat{w}$, $\hat{r}$, *and* $\hat{t}$ are the corresponding dimensional variables. One chose to use $\sqrt{\delta_{OD}}, \sqrt{\delta_{OA}}$ in Eq. (1) due to the fact that δ_{OD}, δ_{OA} are the dimensionless excitation force coefficient from the DC and AC voltage applied. The dimensionless parameters from Eq. (1) are μ the dimensionless damping coefficient, δ_{OD} and δ_{OA} are the dimensionless excitation force coefficients, and Ω the dimensionless excitation frequency, given by

$$\mu = 2c_1\sqrt{\frac{R^4}{\rho h D}},\quad \delta_{OD}=\frac{R^4\varepsilon^* V_{OD}^2}{2Dd^3},\quad \delta_{OA}=\frac{R^4\varepsilon^* V_{OA}^2}{2Dd^3}$$
$$\Omega = \Omega^*\sqrt{\frac{\rho h R^4}{D}},\quad D=\frac{Eh^3}{12\left(1-\nu^2\right)} \tag{3}$$

where ρ is density of plate material, *h* is the thickness of the plates, c_1 is the damping coefficient, *d* is the distance between the plates, ε* is the permittivity of air, *E* is Young's modulus of the material of the plates, ν is the Poisson's ratio of the material, and Ω^* the dimensional excitation frequency

As shown in Eq. (1), the electrostatic force acting on the circular plate is proportional to the square of cosine of the excitation frequency. Therefore the electrostatic force includes a component proportional to the cosine of double the AC frequency. In conclusion, when the system is actuated with an AC frequency near natural frequency of the plate, the electrostatic force experienced by the plate has a frequency near twice natural frequency of the plate, resulting in parametric resonance.

REDUCED ORDER MODEL

The reduced order model (ROM) method is used to model the MEMS clamped circular plate. This method uses the undamped linear mode shapes of the plate based on the Galerkin procedure. The solution is assumed

$$w(r,t)=\sum_{i=1}^{N} w_i(t)\phi_i(r) \tag{4}$$

where the number of terms *N* is finite, dimensionless displacement $w(r,t)$ is a function of a time-dependent coefficient of displacement $w_i(t)$ and the mode shape $\phi_i(r)$. The mode shapes satisfy the boundary conditions of fixed plate i.e. $\phi_i(1)=0$ and $\phi_i'(1)=0$, and the orthogonality conditions.

$$\phi_i^{(4)}+\frac{2}{r}\phi_i'''-\frac{1}{r^2}\phi_i''+\frac{1}{r^3}\phi_i'=\omega_i^2\phi_i' \tag{5}$$

$$\int_0^1 r\phi_i\phi_j dz=\delta_{ij}=\begin{cases}0 & ,i\neq j\\ 1 & ,i=j\end{cases} \tag{6}$$

The partial differential equation of motion Eq. (1) is multiplied by $(1-w)^2$ to eliminate all displacement terms from the denominator. The equation is then expanded and derives into

$$\begin{aligned}&\left(w^2-2w+1\right)\frac{\partial^2 w}{\partial t^2}+\left(w^2-2w+1\right)\mu\frac{\partial w}{\partial t}\\&+\left(w^2-2w+1\right)\left[w^{(4)}+\frac{2}{r}w^{(3)}-\frac{1}{r^2}w^{(2)}+\frac{1}{r^3}w^{(1)}\right]\\&=\delta_{OD}+2\sqrt{\delta_{OD}\delta_{OA}}cos\Omega o+\delta_{OA}cos^2\Omega t\end{aligned} \tag{7}$$

ROM can be used to model the system at any range of frequency. The AC frequency used in this paper is near half the natural frequency, the excitation frequency Ω becomes

$$\Omega=\frac{\omega_1}{2}+\sigma \tag{8}$$

where σ is a detuning parameter. Applying Eq. (4) (5) and (6) into Eq. (1) results in

$$\begin{aligned}&\sum_{i=1}^{N}\frac{\partial^2 w_i}{\partial t^2}\left(\int_0^1 r\phi_n\phi_i dz-2\sum_{j=1}^{N}w_j\int_0^1 r\phi_n\phi_i\phi_j dz\right)+\\&\sum_{i=1}^{N}\frac{\partial^2 w_i}{\partial t^2}\left(\sum_{jk}^{N}w_j w_k\int_0^1 r\phi_n\phi_i\phi_j\phi_k dz\right)=\\&-\mu(\sum_{i=1}^{N}\frac{\partial w_i}{\partial t}\int_0^1 r\phi_n\phi_i dz-2\sum_{ij}^{N}\frac{\partial w_i}{\partial t}w_j\int_0^1 r\phi_n\phi_i\phi_j dz\\&+\sum_{ijk}^{N}\frac{\partial w_i}{\partial t}w_j w_k\int_0^1 r\phi_n\phi_i\phi_j\phi_k dz)-\sum_{i=1}^{N}\omega_i^2 w_i\int_0^1 r\phi_n\phi_i dz\\&+2\sum_{ij}^{N}\omega_i^2 w_i w_j\int_0^1 r\phi_n\phi_i\phi_j dz-\sum_{ijk}^{N}\omega_i^2 w_i w_j w_k\int_0^1 r\phi_n\phi_i\phi_j\phi_k dz\\&+\delta_{OD}\int_0^1 r\phi_n+\delta_{OA}\int_0^1 r\phi_n dz\cos^2(\Omega t)\end{aligned} \tag{9}$$

where n = 1,2,…N.

$$\begin{aligned} y(1) &= w_1 & \dot{y}(1) &= y(2) \\ y(2) &= \dot{w}_1 \quad \Rightarrow & \dot{y}(2) &= \ddot{w}_1 \\ y(3) &= w_2 & \dot{y}(3) &= y(4) \\ y(4) &= \dot{w}_2 & \dot{y}(4) &= \ddot{w}_2 \end{aligned} \tag{8}$$

The resulting system of N second order differential equations is then integrated using AUTO-07p software. The convergence of the responses based on the number of terms N is investigated for both amplitude-frequency response.

RESULTS AND DISCUSSION

The first seven dimensionless mode shape constants along with their corresponding natural frequencies are shown in Table 1. The system constants used by the equation of motion are shown in Table 2. Table 3 and Table 4 show the dimensional and the derived dimensionless system parameters used for numerical simulations.

Table 1. Natural Frequencies of Clamped Circular Plates

Mode	1	2	3	4	5	6	7
Freq.	10.22	39.77	89.10	158.18	247.01	355.57	483.87

Table 2. System Constants

Permitivity of free space	ε^*	8.854e-12	$C^2/N/m^2$

Table 3. Dimensional System Parameters

Radius of plate	R	250.0	μm
Initial gap distance	d	1.014	μm
Plate thickness	h	3.01	μm
Young's modulus	E	150.6	GPa
Poisson's ratio	v	0.0436	
Density of material	ρ	2330.0	kg/m^3
Damping	c_1	1.962	Ns/ m^3
DC Voltage	V_{OD}	0.1438	V
AC Voltage	V_{OA}	2.035	V

Table 4. Dimensionless System Parameters

Electrostatic constant (DC Volt.)	δ_{OD}	0.001
Electrostatic constant (AC Volt.)	δ_{OA}	0.200
Damping constant	μ	0.005

The frequency response of the system is shown in Figure 2. The response is separated into two branches, left and right, where the solid represents the system in a stable state and the dashed lines represent the system in an unstable state (pull-in). One can notice the existence of two saddle-node bifurcation points one in lower frequency and lower amplitude, and another one in higher frequency and higher amplitude. Bifurcation points are points where the system changes stability.

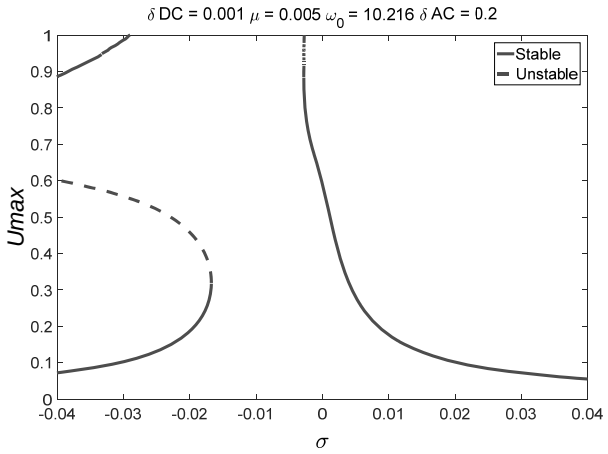

Fig. 2. Frequency response using 2 term ROM. The Bifurcation point is indicated by a dotted line. δ_{OD}= 0.001, δ_{OA}= 0.2, μ = 0.005.

Figure 3 shows the influence of the AC voltage on the frequency response of the system. The right branch of the response does not change greatly as the AC voltage changes, while the left branch shifts significantly to lower frequencies. The increasing AC voltage causes a shift in the left branch of the response to lower frequencies which also increases the gap between the two branches. The amplitudes of the bifurcation points do not seem to be affected by the change in AC voltage.

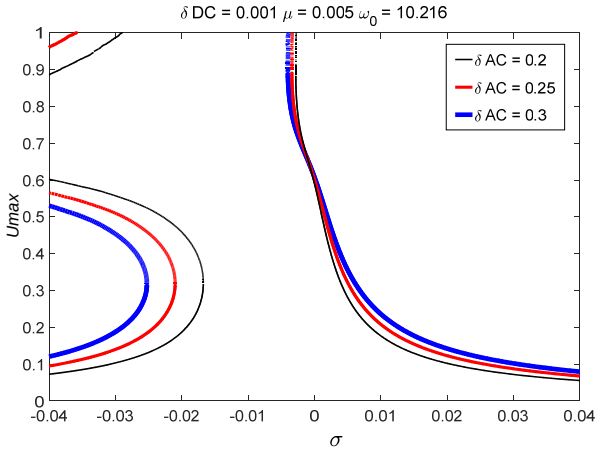

Fig. 3. AC effect on frequency response using 2 term ROM. δ_{OD}= 0.001 and μ= 0.005.

Figure 4 shows influence of the DC voltage on the frequency response of the system. This figure shows a clear softening effect of the response as the voltage is increased. Unlike the AC voltage influence, DC voltage does affect both branches of the response. The right branch leans to towards lower frequency which decreases the gap between branches as the voltage is increased. The bifurcation point occurring at high amplitudes is also shifted to lower frequencies and amplitudes. The left branch is affected similarly like it was from AC voltage. Both bifurcation points are shifted to lower amplitudes.

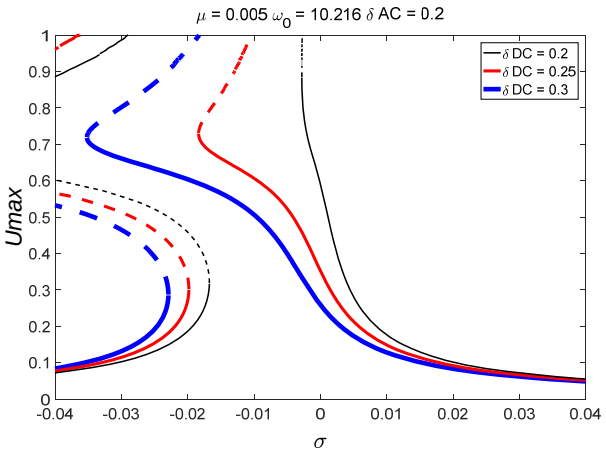

Fig. 4. DC effect on frequency response using 2 term ROM. δ_{OA}= 0.2 and μ= 0.005.

Figure 5 shows the influence of the damping on the frequency response of the system. As the damping increases, the bifurcation points get closer to each other until both branches coalesce. The damping effect on the response is unlike the voltage influence. At the highest damping considered, the system experiences linear behavior. There is a softening effect that can be seen as the damping is increased, even when the behavior becomes linear the response is leaning towards the left.

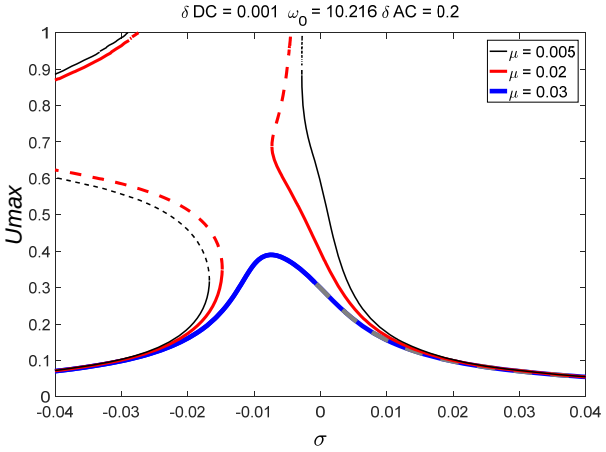

Fig. 5. Damping effect on frequency response using 2 term ROM. δ_{OD}= 0.001 and δ_{OA}= 0.2.

A potential engineering application of this work is in the mass sensing area. Sensors can be designed to work at one fourth of the natural frequency of the structure.

REFERENCES

[1] Zhou, S., Sheng, L., Shen, Z., 2014, "Transverse vibration of circular graphene sheet-based mass sensor via nonlocal Kirchhoff plate theory," Computational Materials Science, Vol. 86, pp. 73-78.

[2] Talebian, S., Rezazadeh, G., Fathalilou, M., Toosi, B., 2010, "Effect of temperature on pull-in voltage and natural frequency of an electrostatically actuated microplate," Mechatronics, Vol. 20, No.6, pp. 666-673.

[3] Farokhi, H., Ghayesh, M., Hussain, S., 2016, "Pull-in characteristics of electrically actuated MEMS arches," Mechanism and Machine Theory, Vol. 98, pp. 133-150.

[4] Lin, M., Chen, R., 2004, "Effect of gradient residual stress on adhesion for a center-anchored circular plate and its underlying substrate," Sensors and Actuators A, Vol. 115, No. 1, 109-117.

[5] Mukherjee, S., Bao, Z., Roman, M., Aubry, N., 2005, "Nonlinear mechanics of MEMS plates with total lagrangian approach," Computers and Structures, Vol. 83, No. 10-11, pp. 758-768.

[6] Pulskamp, J., Bedair, S., Polcawich, R., Smith, G., Martin, J., Power, B., Bhave, S., 2012, "Electrode-shaping for the excitation and detection of permitted arbitrary modes in arbitrary geometries in piezoelectric resonators," IEEE Transactions of Ultrasonics, Ferroeelctrics, and Frequency Control, Vol. 59, No. 5, pp. 1043-1060.

[7] Zhong, Z., Zhang, W., Meng, G., Wang, M., 2015, "Thermoelastic Damping in the size-dependent microplate resonators based on modified couple stress theory," Journal of Microelectromechanical Systems, Vol. 24, No. 2, pp. 431-445.

[8] Caruntu, D., Taylor, K., 2014, "Bifurcation type change of AC electrostatically actuated MEMS resonators due to DC bias," Shock and Vibration, Vol. 2014, No. 542023, pp. 1-9.

[9] Wang, K., Kitamura, T., Wang, B., 2015, "Nonlinear pull-in instability and free vibration of micro/nanoscale plates with surface energy- A modified couple stress theory model," International Journal of Mechanical Sciences, Vol. 99, pp. 288-296.

[10] Li, Z., Zhao, L., Ye, Z., Wang, H., Jiang, Z., & Zhao, Y., 2013, "Resonant Frequency Analysis on an Electrostatically Actuated Microplate under Uniform Hydrostatic Pressure," Journal of Physics D: Applied Physics, Vol. 46, No. 19, pp. 1-7.

[11] Batra, R., Porfiri, M., Spinello, D., 2008, "Reduced order models for microelectromechanical rectangular and circular plates incorporating the Casimir force," International Journal of Solids and Structures, Vol. 45, No. 11-12, pp. 3558-3583.